Published in final edited form as:
IEEE Trans Magn. 2013 February ; 49(1): 309–315.

Open Gradient Magnetic Red Blood Cell Sorter Evaluation on Model Cell Mixtures

Lee R. Moore[1], **Franzisca Nehl**[1,2], **Jenny Dorn**[1,2], **Jeffrey J. Chalmers**[3], and **Maciej Zborowski**[1]

[1]Lerner Research Institute, Cleveland Clinic, Cleveland, OH 44195 USA

[2]Technische Universität Dresden, Fakultät Maschinenwesen/Bioverfahrenstechnik, Dresden, Germany

[3]William G. Lowrie Department of Chemical and Biomolecular Engineering, The Ohio State University, Columbus, OH 43210 USA

Abstract

The emerging applications of biological cell separation to rare circulating tumor cell (CTC) detection and separation from blood rely on efficient methods of red blood cell (RBC) debulking. The two most widely used methods of centrifugation and RBC lysis have been associated with the concomitant significant losses of the cells of interest (such as progenitor cells or circulating tumor cells). Moreover, RBC centrifugation and lysis are not well adapted to the emerging diagnostic applications, relying on microfluidics and micro-scale total analytical systems. Therefore, magnetic RBC separation appears a logical alternative considering the high iron content of the RBC (normal mean 105 fg) as compared to the white blood cell iron content (normal mean 1.6 fg). The typical magnetic forces acting on a RBC are small, however, as compared to typical forces associated with centrifugation or the forces acting on synthetic magnetic nanoparticles used in current magnetic cell separations. This requires a significant effort in designing and fabricating a practical magnetic RBC separator. Applying advanced designs to the low cost, high power permanent magnets currently available, and building on the accumulated knowledge of the immunomagnetic cell separation methods and devices, an open gradient magnetic red blood cell (RBC) sorter was designed, fabricated and tested on label-free cell mixtures, with potential applications to RBC debulking from whole blood samples intended for diagnostic tests.

Index Terms

Magnetic susceptibility; Biomagnetics; Permanent magnets; Cellular biophysics; Fluid dynamics

I. Introduction

The mainstay RBC separation technique is differential centrifugal sedimentation based on the characteristically higher RBC density relative to other blood cells. There are many advantages of centrifugal RBC separation as attested by its continuous use in clinical and

Corresponding author: M. Zborowski (zborowm@ccf.org).

research laboratories for over 50 years. However, this classical technique has drawbacks which become apparent in many of the proposed diagnostic devices, such as the emerging microfluidic applications and devices [1, 2]. For these new applications to be user friendly and inexpensive, it would be ideal to replace the relatively expensive and cumbersome centrifugation step with a label-free, magnetic step. Examples of such non-centrifugal, label-free magnetic separations on a “chip” have recently been reported [3, 4]. Therefore, we have evaluated a different principle for the RBC separation from blood based on cell magnetophoresis, and designed, built and tested a laboratory prototype magnetic RBC separator for low blood sample volume applications. RBC magnetophoresis is the cell motion in suspension induced by an applied magnetic field. We have measured the *intrinsic* (label-free) RBC magnetophoretic mobility (MM) in the course of previous studies using a technique referred to as cell tracking velocimetry (CTV), and have shown that it depends on the presence of high-spin hemoglobin in the cell [5]. In the presence of oxygen in solution, the electron spin of the oxygen-heme complex with the adjacent globin bonds has zero net value, resulting in their null contribution to the total RBC magnetic moment, and leaving the cell slightly more diamagnetic than water because of the globin diamagnetic contribution [6]. In the absence of oxygen, the net electron spin of the four heme groups in the hemoglobin is non-zero, resulting in their collective paramagnetic contribution that is almost equal, but of opposite sign to the total diamagnetic globin contribution, leaving the cell less diamagnetic than water. The net effect is such that the oxygenated RBC’s in solution are pushed away from the magnet (have negative MM value) and the deoxygenated RBC’s are attracted to the magnet (have positive MM value). The effect for the oxygenated RBC’s is very weak and comparable to that of other (non-RBC) cells in the blood (that do not contain hemoglobin), so that they could be considered non-magnetic (MM ≈ 0, Fig. 1). The quantitative measurements of RBC mobility in cell suspension were the basis for engineering design, analysis and fabrication of a laboratory prototype magnetic RBC sorter built from commercially available, block permanent magnets to serve as a test bed for magnetic RBC separation experiments.

II. Materials AND Methods

A. Theory

1) Magnetophoretic mobility (MM)—Magnetophoretic mobility (MM) governs particle transport in viscous media, induced by a magnetic field [7]. Its physical significance is analogous to that of electrophoretic mobility in the description of particle motion in an electric field [8]. It is defined as the ratio of the particle field-induced velocity, u_m, to the local magnetic field energy density gradient, S_m:

$$MM=\frac{u_m}{S_m}=\frac{u_m}{|\nabla\frac{1}{2}HB|}$$

where H and B are magnitudes of the local **H** and **B** fields in the absence of the particle. We have relied on magnetophoretic mobility as a basis of continuous magnetic cell sorting methods and instrumentation during our past studies [10, 11]. The high sensitivity of the CTV technique to single cell motion allowed us to determine the relationship between

surface antigen expression and the immunomagnetic superparamagnetic iron oxide (SPION) label binding [9], and to measure the difference in the MM distributions between RBCs differing in the hemoglobin magnetic moment [5]. The different MM obtained for paramagnetic and non-paramagnetic erythrocytes agreed with values calculated on the basis of bulk hemoglobin content and red blood cell magnetic susceptibility measurements by Gouy's method [11], superconducting quantum interference device (SQUID) [12] and nuclear magnetic resonance (NMR) methods [13]. For the typical values of an average magnetic field of 1.5 T and gradient of 100 T/m in the CTV analyzer, and the mean MM of the deoxygenated RBC, shown in Fig. 1, corresponds to the mean velocity of 1.2 μm/s.

2) Magnetic centrifuge—For practical purposes, centrifugal acceleration in laboratory centrifuges is quoted in multiples of the standard gravitational acceleration, or "number of *g*'s". In typical laboratory applications, the RBC fraction is separated from whole blood by applying a centrifugal field of 300× *g* to 400× *g* for between 15 and 5 min, respectively. The dependence of the field-induced velocity of the RBC, u_m, on its magnetic susceptibility relative to that of the carrier fluid, $\chi_{RBC} - \chi_{fluid}$, is mathematically similar to the dependence of the RBC sedimentation velocity, u_g, on its mass density relative to that of the fluid, $\rho_{RBC} - \rho_{fluid}$, and therefore:

$$\frac{u_m}{u_g} = \frac{\chi_{RBC} - \chi_{fluid}}{\rho_{RBC} - \rho_{fluid}} \frac{S_m}{g}$$

where g = 9.81 m/s^2 is the standard gravitational acceleration [14]. (Note that, in general, the volume magnetic susceptibility is equal to the mass, or specific, magnetic susceptibility times mass density of the substance, which upon substitution in the above equation, results in a dimensionless ratio of the mass susceptibility difference over mass density difference on the right-hand side of the equation.) Given that one measure of the effectiveness of a separation technology is the magnitude of the field-induced velocity, the inspection of the above equation allows one to directly compare centrifugal to magnetic separation. For example, the density difference between a RBC and typical suspending buffer is 84 kg/m^3, whereas the difference in the volume magnetic susceptibility between a RBC and suspending buffer is on the order of 5×10^{-6} (Table 1). This indicates that an absolute value of S_m of seven orders of magnitude higher than standard gravity is needed to achieve a 1:1 ratio of the magnetic field-induced velocity to the gravitational settling velocity for RBCs in aqueous suspensions. We have previously reported on magnet designs that are capable of $S_m = 1.2\times10^8$ T·A/m^2. Here we provide initial experimental data for a design of $S_m = 2.0\times10^9$ T·A/m^2 evaluated at the magnet surface. In addition, the effect of low magnetic migration velocity, u_m, is compensated for by a much shorter travel distance, ~100 μm to achieve the RBC separation (Fig. 2) than that in a typical laboratory centrifuge, ~10 cm [15, 16]. The values of key design parameters are summarized in Table 1.

3) Magnetic pressure and viscous flow shear stress—The magnetic field, **H**, was modeled either by using closed form formulas for rectangular block permanent magnets arranged to produce an idealized quadrupole field [17], or using a commercial engineering software package to simulate the field of the actual steel and permanent magnets in the

manufactured magnet assembly (2D Magneto and 3D Amperes, from Integrated Engineering Software IES, Winnipeg, Manitoba, Canada). The closed form approximation was used to visualize the magnetic deposition of the paramagnetic (reduced) RBCs inside a cylindrical tube of the "magnetic centrifuge" immersed in the quadrupole field, and to visualize the competing effect of the viscous flow shear stress that causes cell wash-off from the cylinder wall due to the imposed flow of the cell suspension through the annular flow channel [17]. Mathematically, the magnetic deposition was visualized as an isosurface on which the magnetic pressure, p_m, was equal to the local viscous flow shear stress, τ_{zr}:

$$p_m=\tau_{zr}, \text{where} \quad p_m=\frac{1}{2}MB, \quad \tau_{zr}=\eta\frac{dv_z}{dr}$$

and

$$M=\Delta\chi H=(\chi_{RBC}-\chi_{H2O})H(x,y,z)$$
$$B=\mu_0 H(x,y,z)$$
$$v_z=v_z(\rho)=\frac{2\langle v_z\rangle}{1+\rho_i^2-\frac{1-\rho_i^2}{\ln(1/\rho_i)}}\left(1-\rho^2+\frac{1-\rho_i^2}{\ln(1/\rho_i)}\ln(p)\right)$$

where v_z is the axial flow velocity of the fluid through the annular channel formed by two co-axial cylinders inserted into the quadrupole magnet aperture (Fig. 2), ρ is the dimensionless radius equal to r/r_o, which for the case of the inner wall of the annulus, $\rho_i = r_i/r_o$, $\langle v_z\rangle = Q/A$ is the mean flow velocity in the channel (equal to the ratio of the volumetric flow rate, Q to the annular channel cross section, A), $r=\sqrt{x^2+y^2}$ and r_o and r_i are the outer and inner cylinder channel radii, respectively [16, 19]. The magnetization M entering the expression for the magnetic pressure, p_m above, is the net magnetization of the RBC relative to that of water, whereas the local magnetic field B is approximated by the expression for the free space because of negligibly small values of χ_{RBC} and χ_{H2O} as compared to unity. The numerical values of constants entering equations, above, are provided in Table 1. The appearance of the magnetic pressure term in the generalized Navier-Stokes equation governing flow of viscous, magnetically susceptible fluids is discussed in [20].

The sum of magnetic pressure and the viscous flow shear stress provided an intuitive picture of the interplay between the RBC magnetic deposition and the RBC wash-off due to the fluid flow (Fig. 3) and aided in the initial selection of volumetric flow of the cell suspension through the magnet.

B. Experiment

1) High quadrupole field from stock permanent magnets—For an ideal quadrupole field, a hyperbolic-shape pole tip is indicated, but we chose flat pole faces to take advantage of lower fabrication cost and the availability of high energy product, stock permanent magnet blocks from commercial suppliers (permitting some field non-uniformity). The permanent magnet blocks are readily available from online retailers, such as K&J Magnetics (Jamison, PA). These are nickel-plated neodymium-iron-boron (Nd-Fe-B) of energy product

42 MGOe. The specific magnet blocks were chosen under three criteria: 1) The overall arrangement of a quadrant grouping should approximate a half-trapezoid, the shape determined to yield the highest aperture flux density per unit magnet cross-section; 2) The thickness of the thinnest block should be such that it approximates the side of a regular octagon (Figs. 2), whose dimension is dictated by the compatible channel diameter; 3) The axial lengths of each block should be such that an integer number sums to a specified assembly axial length - in this case 3 inches (76.2 mm) - to avoid the need to cut them. In all cases, the magnet blocks were purchased pre-magnetized through their thicknesses and arranged by polarity to yield a quadrupole field, as shown in Fig. 2 and Fig. 6.

2) Experimental setup—The annular flow channel was placed inside the quadrupole magnet and connected to a fluidics system comprising disposable, plastic syringes mounted on syringe pumps, diagonal switching valves, reservoirs for fluid carrier and sample, hardware to sparge nitrogen through the reservoirs (not shown), and an in-line light detector (not shown) used in the initial system optimization (Fig. 4).

The cell suspension was added to the sample container (with a magnetic stirrer that kept the cells in suspension for the entire injection process). Oxygenated RBCs were used as a negative control, and reduced RBCs (method given below) served as a positive control. The time sequence of loading the cell suspension into the magnet, stopping the flow to provide sufficient residence time for the RBCs to migrate to the channel wall, resumption of flow at low flow rate for nonmagnetic fraction elution, followed by high flow rate flush to recover the magnetic fraction, is illustrated in Fig. 5. The sample volume was 0.020 mL; thus, 1.0×10^6 cells were processed per experiment resulting in an average throughput for a 30 min experiment (including deoxygenation) of 3.3×10^4 cells/min.

3) Cell model system—Human whole blood (with addition of citrate phosphate dextrose adenine (CPDA-1) as an anticoagulant) was received from the Cleveland Clinic Blood Banking and Transfusion Medicine lab following therapeutic phlebotomy under an IRB approved protocol. The whole blood was centrifuged (400 g, 5°C for 9 min) and washed (PBS) thrice to replace blood plasma and deplete the RBC preparation of white blood cells and platelets. The RBC hemoglobin was converted to paramagnetic deoxyhemoglobin by exposure to nitrogen atmosphere in the sample container prior to magnetic sorting (Fig. 4). For positive control studies, RBC hemoglobin was reduced to paramagnetic methemoglobin (5mL RBC stock suspension was mixed with 5mL of 10 mM sodium nitrite solution and incubated for about one hour). The KG-1a cell line was purchased from The American Type Culture Collection (ATCC, Manassas, VA). This is a variant subline of the human acute myelogenous leukemia cell line KG-1. The cell line was cultured in Iscove's Modified Dulbecco's Medium (IMDM) with 4 mM L-Glutamine, 10% fetal bovine serum (5% CO2) and 1% Penicillin/Streptomycin (50 units/mL; 50 μg/mL). The cell cultures were incubated for at least 2 weeks at 37°C and 5% CO_2 saturation while replacing the culture media every third day. The IMDM was purchased from ATCC (Manassas, VA), whereas FBS and Penicillin/Streptomycin were provided by the Cell Culture Core at the Cleveland Clinic. The RBCs were mixed in equal proportion with the KG-1a cells and adjusted to a final number

concentration of approximately 0.5×10^8/mL as a model for hematopoietic stem cell culture conditions [21]. Cells were counted (in triplicate) using a hemacytometer.

III. Results

A. Magnet construction and field measurements

The pole pieces and blocks combine to form a square quadrant component of the permanent magnet assembly (Fig. 6). The aperture width, the distance between opposing faces of the octagon, is 1.9 mm. The assembly of magnet blocks and pole pieces are held in place with 3/16" (4.76 mm) thick aluminum plates forming an outer shell (labeled "C" in Fig. 6). A cross-section through the geometry with overlaid *B* field color contours is indeed characteristic of a quadrupole field (Fig. 2).

The impact of angle and axial position *z* at fixed $r = r_o$ on *B* is shown in Figure 7. The data is sourced from the output of Amperes, calibrated to match gaussmeter measurements. The interval from 0 to 45 degrees is sufficient to portray the entire aperture, due to symmetry. Thus, B_0 (the average *B* evaluated at r_o) was found to be 1.55 T.

B. Cell sorting results

The cell sorting experiments were performed using sequential fraction collection at low flow rate ("eluate") and high flow rate ("retentate") pump operation (Fig. 8). The initial experiments were performed on the positive control (paramagnetic methemoglobin RBCs) and the negative control (diamagnetic oxyhemoglobin RBCs) cells to confirm the theoretically predicted volumetric flow rates required for the highest cell fraction recoveries (Fig. 8).

Most of the paramagnetic met RBC were collected in the retentate fraction (as expected of the "magnetic" cells), whereas most of the oxy RBC were collected in the eluate fraction (as expected of the "non-magnetic" cells), Fig. 8. Subsequently, the magnetic RBC separator was tested on a mixture of deoxygenated RBC's (deoxy RBC) and the white blood cell line (KG1-a) mixed in equal numbers. The white blood cell line separated from the deoxy RBCs in the eluate fraction (with only few cells counted in the retentate), whereas most of the RBC's were collected in the retentate fraction, Fig. 9. These results confirmed the feasibility of the RBC separation in an open gradient magnetic sorter and provided a basis for scaled-up sorter designs.

IV. Discussion

Erythrocytes are an ideal cell model for label-free magnetic separation, because their structure is relatively simple and physical parameters, such as diameter, volume and hemoglobin contents, are homogeneous in the population of a particular individual [22, 23]. Melville and co-workers showed in the mid 1970's the capture of erythrocytes, reduced after treatment with a sodium dithionite solution, using a ferromagnetic wire mesh in a high gradient magnetic separator (HGMS) with wire magnetized by an external magnetic field [21]. Later, Owen showed that RBC capture was also possible by conversion to methemoglobin RBC [22].

The HGMS columns were the precursors of the immunomagnetic cell separation columns commercially available today, in which cell selection is achieved with the use of monoclonal antibodies linked to superparamagnetic iron oxide nanoparticles (SPIONs) [26, 27]. It is interesting to note that the currently FDA approved, circulating tumor cell (CTC) detection method (for breast, colorectal and prostate cancers) is firmly based on magnetic cell separation without using centrifugation or hemolysis for sample preparation (Veridex LLC, a Johnson & Johnson Company)]. Label-free magnetic RBC separation may simplify sample preparation over current methods requiring immunomagnetic labeling with SPIONs. The RBC retention in a large volume of blood inserted into a superconducting NMR magnet has been studied [28]. Separation of white blood cells (WBC's) rather than RBC's, based on their diamagnetic repulsion in a single-wire HGMS configuration, has been described [29] based on earlier studies on a continuous selective HGMS in the repulsive force mode. Lack of RBC capture in HGMS arrays, proposed recently for labeled cell magnetic separation was noted [30]. However, there is a renewed interest in magnetic RBC separation on a small scale because of the enabling microfabrication technologies based on micro-electromechanical systems (MEMS) [2, 3, 4, 31, 32] and a potential for improved rare CTC recovery over current methods [33].

The open-gradient magnetic separation presented here is aided by the fluid mechanics of the viscous suspension flow due to non-magnetic cell radial drift away from the channel walls occurring in Poiseuille flow in straight, cylindrical channels [35]. The behavior of cells and other microparticles in viscous flow has been a subject of numerous experimental and theoretical studies [36–38]. Blood rheology has many different interesting properties that set it apart from an ordinary Newtonian fluid [39]. In particular, for a cell in contact with a solid surface, the shear flow causes cells to lift and move away from the surface even at low channel Reynolds number [40]. Such effects may oppose retention of non-magnetic cells in the magnetic sorter and improve RBC purity in the magnetic fraction. Interestingly, the extent of the cell migration in a shear flow made it practical to propose a purely microfluidic depletion of RBCs from whole blood in high aspect ratio microchannels [41]. We have recently analyzed the importance of shear-induced microparticle diffusion in laminar flow suspensions [42]. The approach was applied here to develop a simple but useful model to visualize the effect of increasing flow rate through the annular channel on the magnetic RBC deposition on the channel wall (Fig. 3). The model was limited to directly equating the energy density of the viscous flow shear stress (in Pa) to the magnetostatic energy density available to hold the magnetic RBC at the magnetic deposition surface (in J/m^3 = Pa). The simulations resulted in a qualitative agreement between theory and experiment, and provided the basis for improved visualization approaches to include secondary effects (such as the finite cell size). In the final analysis, based on the experimental parameters summarized here (Table 1), we have demonstrated the feasibility of label-free magnetic RBC separation from mixed cell suspensions in open-gradient magnetic field using a small volume laboratory prototype magnetic RBC sorter. The cell number throughput (3.3×10^4/min $\approx 2\times10^5$/h) was higher than that (1×10^5/h) recently reported for a label-free magnetic sorting (albeit for different flow and magnetic field configurations) [4]. It was obviously much lower as compared to the capabilities of a state-of-the-art centrifugal RBC separation (on the order of 10^9/min). Nevertheless, considering the potential of the magnetic

RBC sorting for an in-line, uninterrupted operation for downstream analysis in microfluidic channels, and a potential for scale-up with increasing channel and magnet dimensions, such sorting may become superior to centrifugation in specialized applications to small volume analytes, such as CTC detection [30]. The challenges that remain are the ability to create a high magnetic field gradient (on the order of 1,000 T/m) in the volume of the cell sorting channel, and a rapid in-line conversion of low spin hemoglobin to high-spin hemoglobin (by deoxygenation or chemical treatment). Based on our current research (in preparation for publication) it is estimated that an open-gradient RBC sorter based on a practical permanent magnet assembly could be built to deplete the RBCs by a factor of 10,000 (to 0.01% of their original fractional concentration) in under 30 min from 5 mL of whole blood.

V. Conclusion

The rapid progress in permanent magnet materials science allows for the generation of high magnetic energy densities and gradients that were only possible in the past using large electromagnets or superconducting magnets. Their high field energy density and gradients in low volumes are ideally suited for application to label-free magnetic separation of RBCs, for potential replacement of centrifugation in microfluidics applications. The low cost and small sizes of the commercially available permanent magnet blocks make them ideal components of compound structures suitable for RBC separation.

Acknowledgments

We thankfully acknowledge funding of this project by grants NIH CA62349 and DARPA BAA07-21, and the expert technical assistance of Boris Kligman.

References

1. Furlani EP. Magnetophoretic separation of blood cells at the microscale. Journal of Physics D-Applied Physics. 2007; 40:1313–1319.
2. Pamme N. On-chip bioanalysis with magnetic particles. Curr Opin Chem Biol. 2012; 16:436–443. [PubMed: 22682892]
3. Jung Y, Choi Y, Ham KH, Frazier AB. Six-stage cascade paramagnetic mode magnetophoretic separation system for human blood samples. Biomed. Microdevices. 2010; 12:637–645. [PubMed: 20349341]
4. Shen F, Hwang H, Hahn YK, Park JK. Label-Free Separation Using a Tunable Magnetophoretic Repulsion Force. Anal. Chem. 2012; 84:3075–3081. [PubMed: 22380761]
5. Zborowski M, Ostera GR, Moore LR, Milliron S, Chalmers JJ, Schechter AN. Red blood cell magnetophoresis. Biophys J. 2003; 84:2638–2645. [PubMed: 12668472]
6. Pauling L, Coryell CD. The magnetic properties and structure of hemoglobin, oxyhemoglobin and carbonmonoxyhemoglobin. Proc Natl Acad Sci USA. 1936; 22:210–216. [PubMed: 16577697]
7. Zborowski M, Moore LR, Williams PS, Chalmers JJ. Separations based on magnetophoretic mobility. Separation Science and Technology. 2002; 37:3611–3633.
8. Melcher, JR. Continuum Electromechanics. Cambridge, MA: The MIT Press; 1981.
9. Moore LR, Zborowski M, Nakamura M, McCloskey K, Gura S, Zuberi M, Margel S, Chalmers JJ. The use of magnetite-doped polymeric microspheres in calibrating cell tracking velocimetry. J Biochem Biophys Methods. 2000; 44:115–130. [PubMed: 10889282]
10. Nakamura M, Zborowski M, Lasky LC, Margel S, Chalmers JJ. Theoretical and experimental analysis of the accuracy and reproducibility of cell tracking velocimetry. Exp Fluids. 2001; 30:371–380.

11. Pauling L, Coryell C. The magnetic properties of the hemochromogens and related substances. Proc Natl Acad Sci U S A. 1936; 22:159–163. [PubMed: 16588065]
12. Savicki JP, Lang G, Ikeda-Saito M. Magnetic susceptibility of oxy- and carbonmonoxyhemoglobins. Proc Natl Acad Sci U S A. 1984; 81:5417–5419. [PubMed: 6591198]
13. Spees WM, Yablonskiy DA, Oswood MC, Ackerman JJ. Water proton MR properties of human blood at 1.5 Tesla: magnetic susceptibility, T(1), T(2), T*(2), and non-Lorentzian signal behavior. Magn Reson Med. 2001; 45:533–542. [PubMed: 11283978]
14. Jin X, Zhao Y, Richardson A, Moore L, Williams PS, Zborowski M, Chalmers JJ. Differences in magnetically induced motion of diamagnetic, paramagnetic, and superparamagnetic microparticles detected by cell tracking velocimetry. Analyst. 2008; 133:1767–1775. [PubMed: 19082082]
15. Williams PS, Moore LR, Chalmers JJ, Zborowski M. Splitter imperfections in annular split-flow thin separation channels: effect on nonspecific crossover. Anal Chem. 2003; 75:1365–1373. [PubMed: 12659197]
16. Williams PS, Zborowski M, Chalmers JJ. Flow rate optimization for the quadrupole magnetic cell sorter. Anal Chem. 1999; 71:3799–3807. [PubMed: 10489528]
17. Furlani, EP. Permanent Magnet and Electromechanical Devices. Materials, Analysis, and Application. San Diego: Academic Press; 2001.
18. Zborowski M, Moore LR, Williams PS, Chalmers JJ. Magnetic pressure as a scalar representation of field effects in magnetic suspensions. Am Inst Physics Conf Proceedings. 2010; 1311:111–117.
19. Bird, RB.; Stewart, WE.; Lightfoot, EN. Transport Phenomena. New York: John Wiley and Sons; 1960.
20. Rosensweig, RE. Ferrohydrodynamics. Cambridge, MA: Cambridge University Press; 1985.
21. Jin X, Abbot S, Zhang X, Kang L, Voskinarian-Berse V, Zhao R, Kameneva MV, Moore LR, Chalmers JJ, Zborowski M. Erythrocyte Enrichment in Hematopoietic Progenitor Cell Cultures Based on Magnetic Susceptibility of the Hemoglobin. PloSONE. 7:8. e39491.
22. Cerdonio M, Morante S, Torresani D, Vitale S, DeYoung A, Noble RW. Reexamination of the evidence for paramagnetism in oxy- and carbonmonoxyhemoglobins. Proc Natl Acad Sci U S A. 1985; 82:102–103. [PubMed: 2982138]
23. Graham MD. Comparison of volume and surface mechanisms for magnetic filtration of blood cells. Journal de Physique, Colloque C.1. 1984; 45(Suppl.):C1/779–C1/784.
24. Melville D, Paul F, Roath S. Direct magnetic separation of red cells from whole blood. Nature. 1975; 255:706. [PubMed: 1134566]
25. Owen CS. High gradient magnetic separation of erythrocytes. Biophys J. 1978; 22:171–178. [PubMed: 656540]
26. Radbruch A, Mechtold A, Thiel S, Miltenyi S, Pflueger E. High-gradient magnetic sorting. Methods Cell Biol. 1994; 42:387–403. [PubMed: 7533249]
27. Roath S, Thomas TE, Watson JH, Lansdorp PM, Smith RJ, Richards AJ. Specific capture of targeted hematopoietic cells by high gradient magnetic separation by the use of ordered wire array filters and tetrameric antibody complexes linked to a dextran iron particle. Prog Clin Biol Res. 1994; 389:155–163. [PubMed: 7535431]
28. Svoboda J. Separation of red blood cells by magnetic means. Journal of Magnetism and Magnetic Materials. 2000; 220:L103–L105.
29. Takayasu M, Kelland DR, Minervini JV. Feasibility of direct magnetic separation of white cells and plasma from whole blood. IEEE Trans Appl Supercond. 2000; 10:927–930.
30. Chen H, Bockenfeld D, Rempfer D, Kaminski MD, Liu X, Rosengart AJ. Preliminary 3-D analysis of a high gradient magnetic separator for biomedical applications. J. Magnetism and Magnetic Materials. 2008; 320:279–284.
31. Nandy K, Chaudhuri S, Ganguly R, Puri IK. Analytical model for the magnetophoretic capture of magnetic microspheres in microfluidic devices. Journal of Magnetism and Magnetic Materials. 2008; 320:1398–1405.
32. Han KH, Han A, Frazier AB. Microsystems for isolation and electrophysiological analysis of breast cancer cells from blood. Biosensors & Bioelectronics. 2006; 21:1907–1914. [PubMed: 16529922]

33. Lara O, Tong X, Zborowski M, Chalmers JJ. Enrichment of rare cancer cells through depletion of normal cells using density and flow-through, immunomagnetic cell separation. Exp Hematol. 2004; 32:891–904. [PubMed: 15504544]
34. Tibbe AGJ, de Grooth BG, Greve J, Dolan GJ, Rao C, Terstappen LWMM. Magnetic field design for selecting and aligning immunomagnetic labeled cells. Cytometry. 2002; 47:163–172. [PubMed: 11891721]
35. Bayliss LE. The axial drift of the red cells when blood flows in a narrow tube. Journal of Physiology. 1959; 149:593–613. [PubMed: 13797830]
36. Segré G, Silberberg A. Radial particle displacements in Poiseuille flow of suspensions. Nature. 1961; 189:209–210.
37. Saffman PG. The lift on a small sphere in a shear flow. Journal of Fluid Mechanics. 1965; 22:385.
38. Joseph DD, Ocando D. Slip velocity and lift. Journal of Fluid Mechanics. 2002; 454:263–286.
39. Pries AR, Secomb TW, Gaehtgens P. Biophysical aspects of blood flow in the microvasculature. Cardiovascular Research. 1996; 32:654–667. [PubMed: 8915184]
40. Cantat I, Misbah C. Lift force and dynamical unbinding of adhering vesicles under shear flow. Physical Review Letters. 1999; 83:880–883.
41. Jäggi RD, Sandoz R, Effenhauser CS. Microfluidic depletion of red blood cells from whole blood in high-aspect-ratio microchannels. Microfluidics and Nanofluidics. 2007; 3:47–53.
42. Williams PS, Hoyos M, Kurowski P, Salhi D, Moore LR, Zborowski M. Characterization of nonspecific crossover in Split-Flow Thin channel fractionation. Analytical Chemistry. 2008; 80:7105–7115. [PubMed: 18698797]

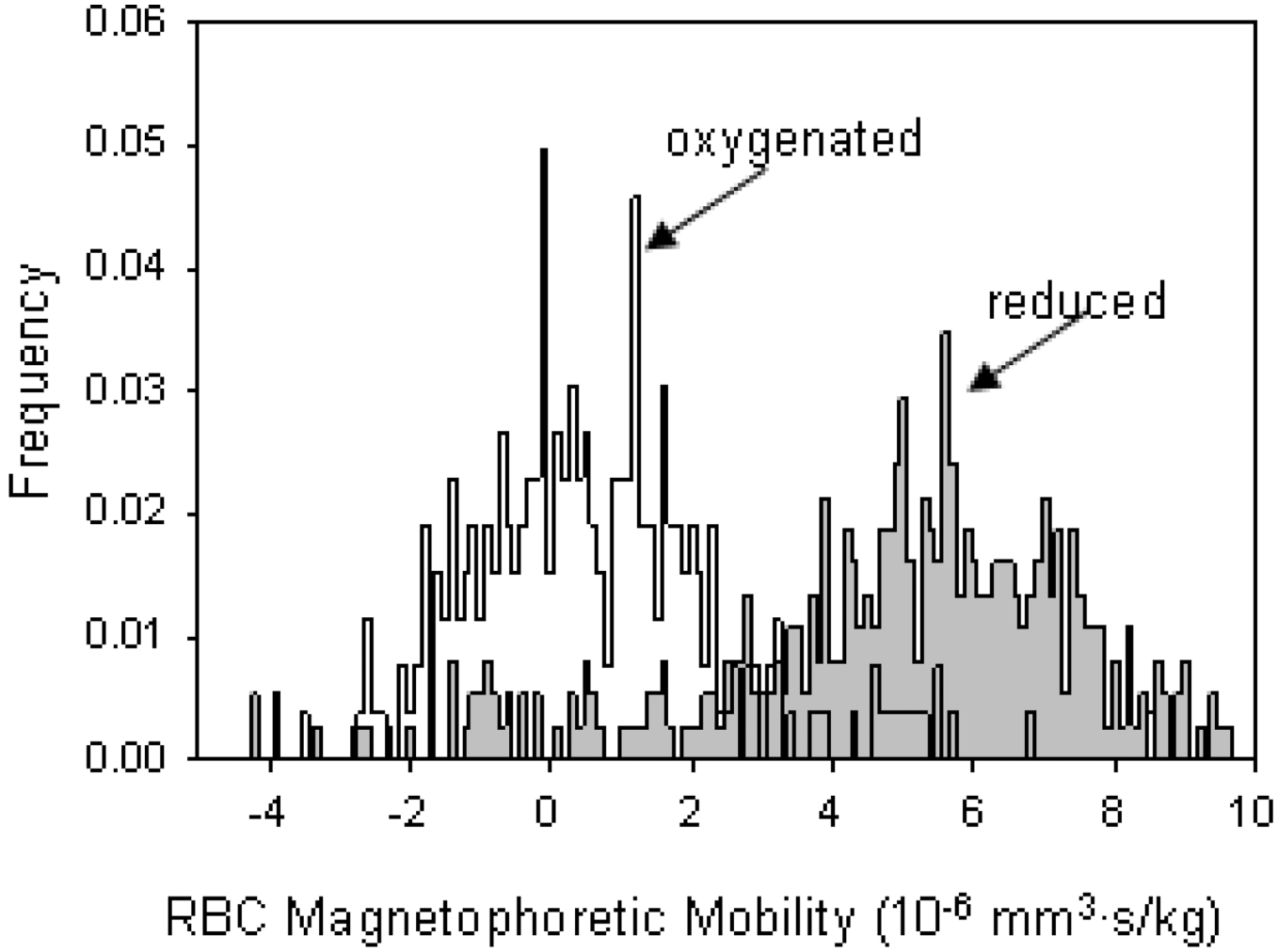

Fig. 1.

Magnetophoretic mobility of reduced RBCs is significantly higher than that of the oxygenated RBCs (used as a negative control), as shown here on mobility histograms generated by Cell Tracking Velocimetry (CTV). The magnetophoretic mobility of the Kg-1a cell line was comparable to that of the oxygenated RBCs (not shown).

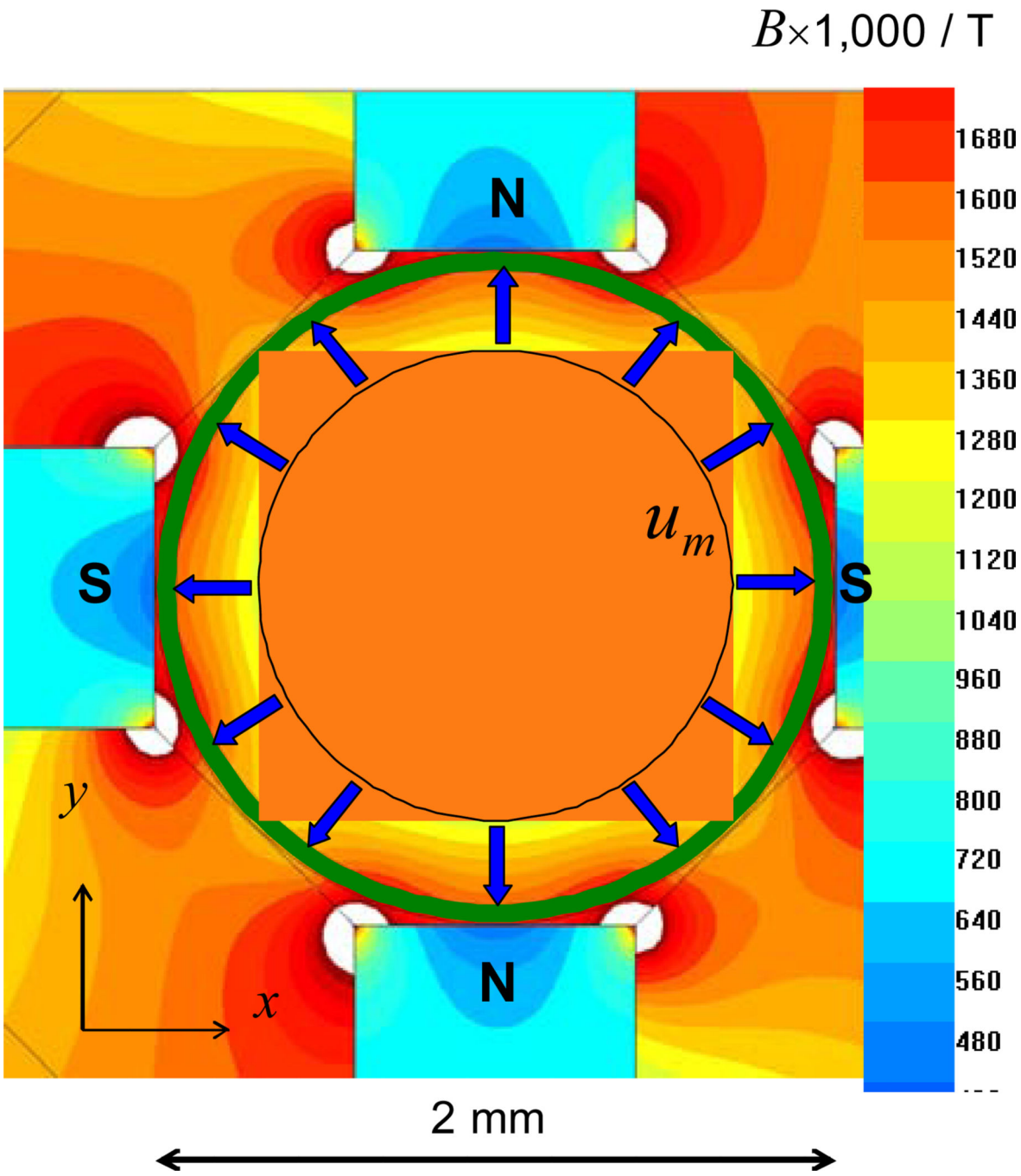

Fig. 2.

Centrifugal distribution of the field-induced RBC (reduced) velocities, u_m, inside the quadrupole magnetic field (deep inside the magnet). The fluid cell suspension was contained between two concentric cylinders forming an annular flow channel of the thickness $r_o - r_i$. The cell suspension mean linear flow velocity along the *z*-axis of the annular channel was matched to u_m allowing sufficient residence time for the RBCs to reach the wall of the outer cylinder.

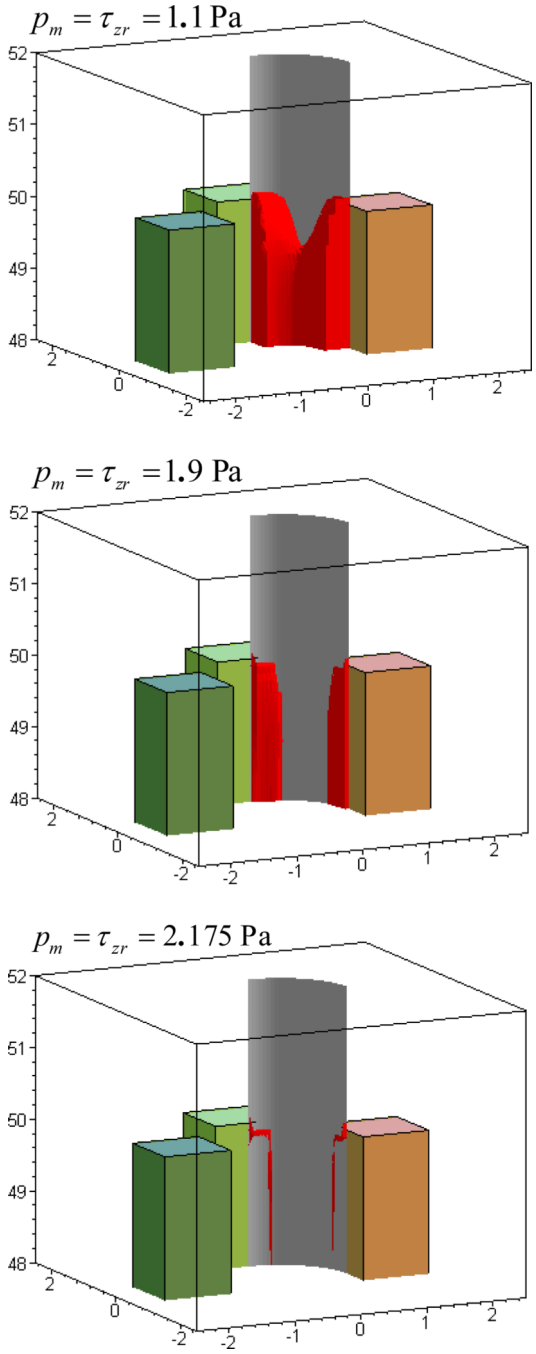

Fig. 3.

The magnetic RBC deposit is washed off of the cylindrical channel wall by the increasing volumetric flow rate of the fluid media (top to bottom), as illustrated by a sequence of local pressure isosurfaces (magnetic = viscous shear, in red). Only three out of four pole pieces, and only a quarter of the channels section are shown, for clarity.

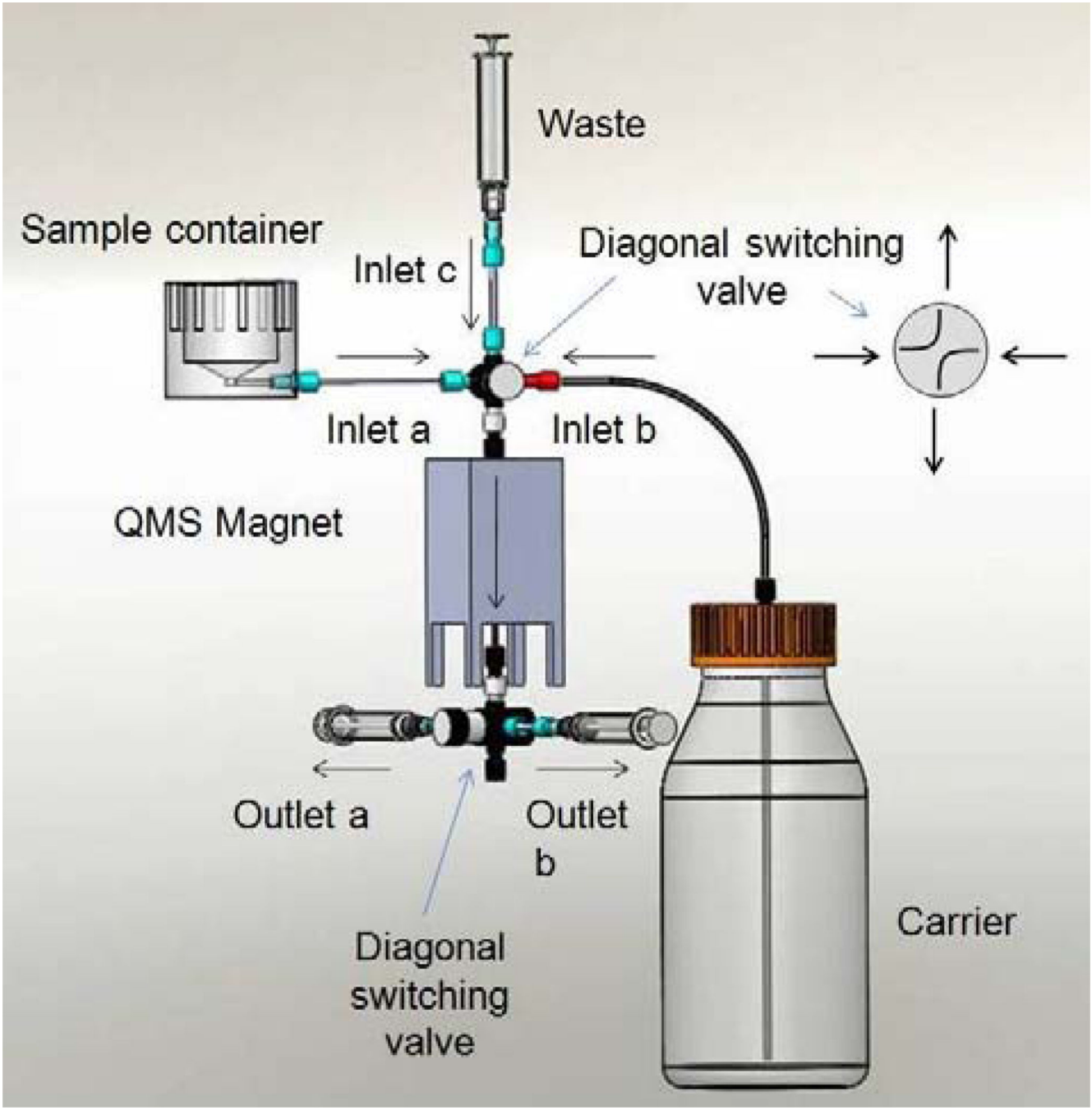

Fig. 4.

Experimental setup showing Quadrupole Magnetic Sorter (QMS) and the associated fluidics system. The fluid flow was driven by two independent syringe pumps (not shown) that were operated alternately at low flow rate (Outlet a, collecting “eluate” fraction at 0.05 mL/min) and high flow rate (Outlet b, collecting “retentate” fraction at 2 mL/min), the flow distributions being controlled by two diagonal switching valves. In selected experiments a light detector was inserted downstream from the QMS for in-line cell elution profile analysis. Here “Carrier” is the carrier fluid media used as a mobile phase. The Sample

container was equipped for operation with the nitrogen gas for RBC hemoglobin conversion to the paramagnetic deoxyhemoglobin.

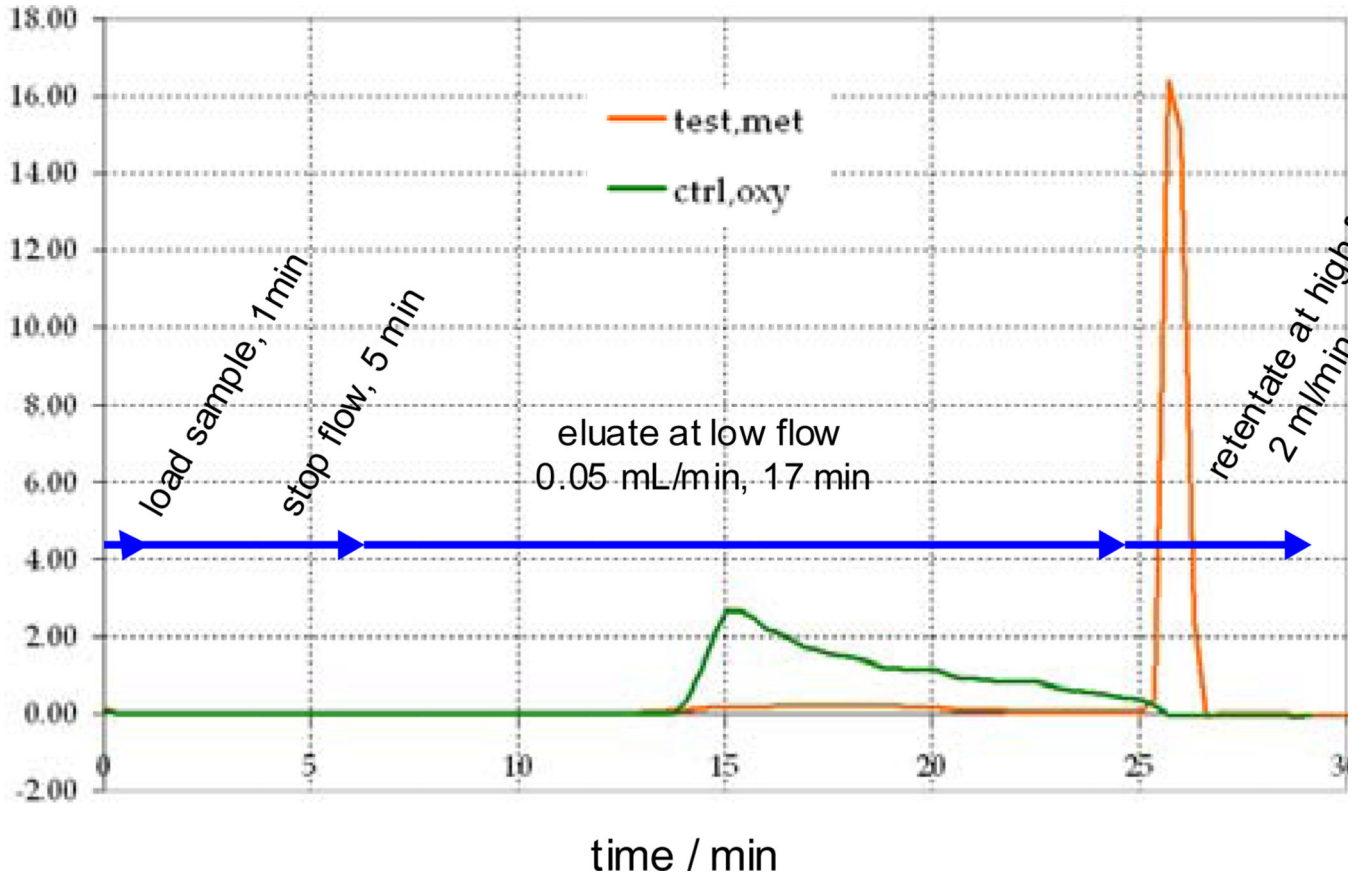

Fig. 5.

Light detector reading following injection of oxygenated RBCs (“ctrl, oxy”) or reduced RBCs (“met, test”) and the time course of sample manipulation in the fluidics system. Note no retention in the magnetic field of oxy RBCs (eluting at low flow rate) and retention of met RBCs (requiring high flow rate for flushing out from the magnet).

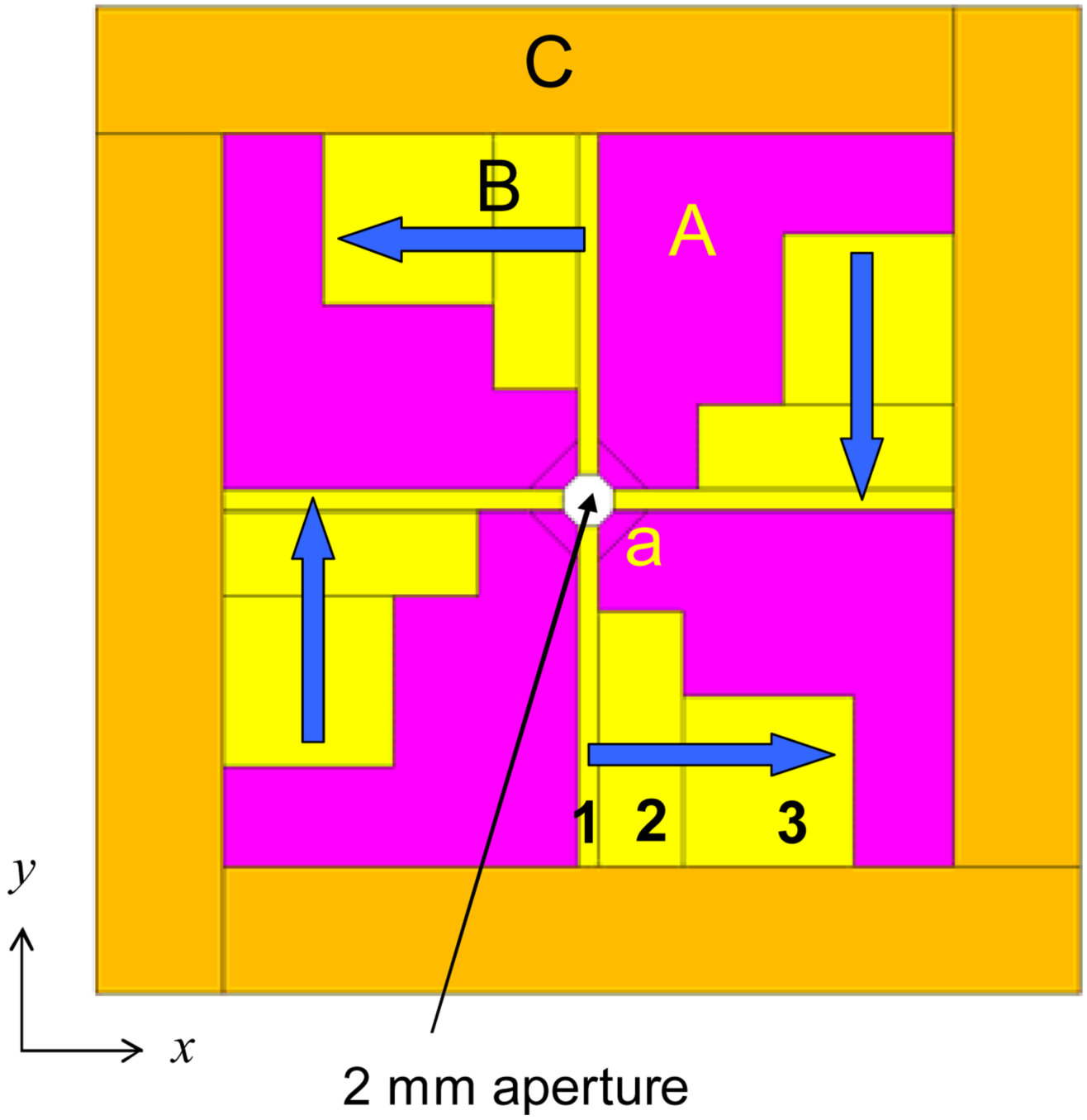

Fig. 6.

High field permanent magnet schematic showing disposition of the commercially available, stock permanent magnet bars (numbered 1, 2, 3, in yellow) embedded in soft iron pieces (magenta) held together by aluminum casing (beige). Blue arrows indicate bar magnets magnetization.

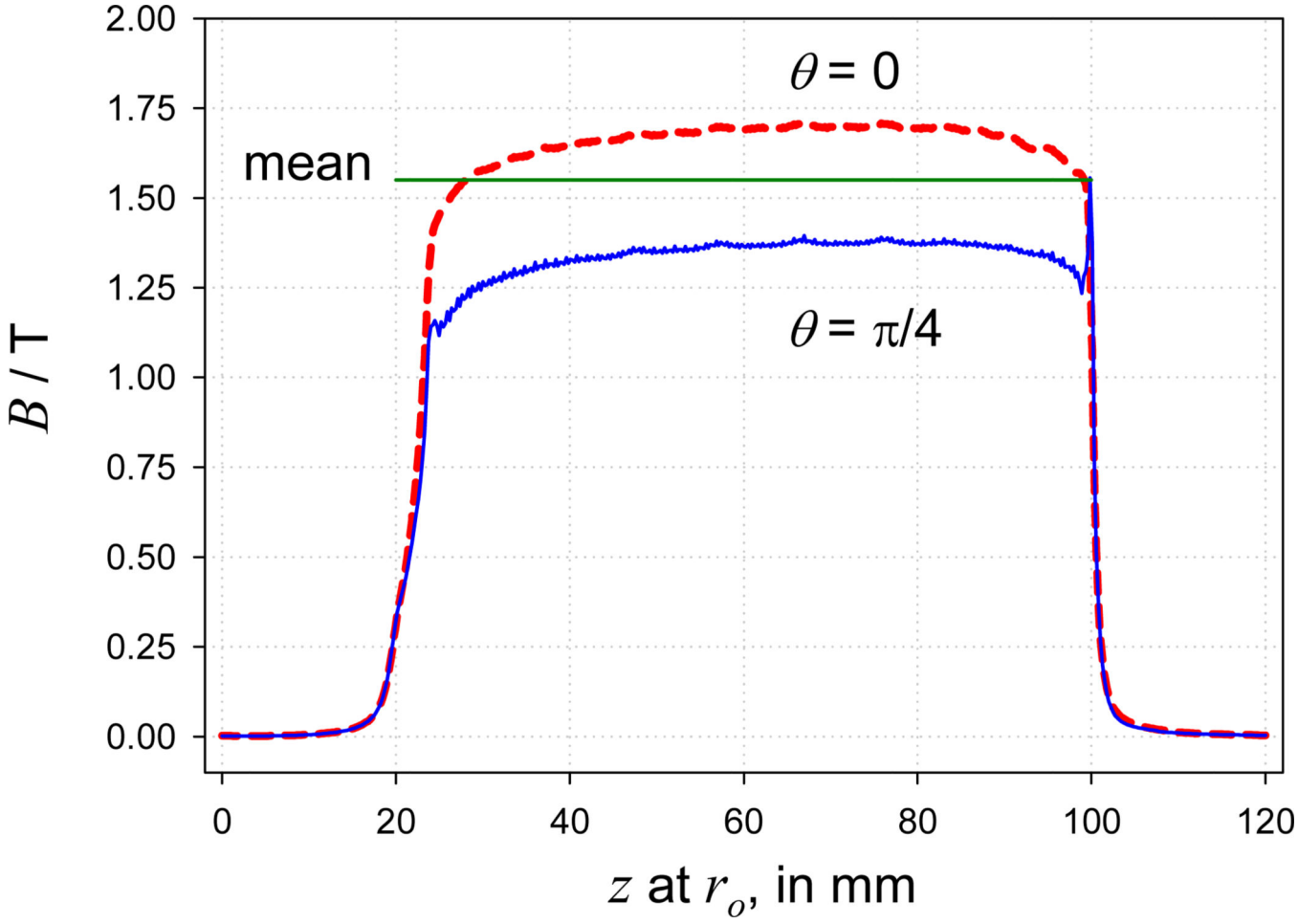

Fig. 7.

Magnetic field calculated along the long axis of the magnet aperture, for two angular coordinates: θ = 0 corresponding to the inside magnet surface, $x = r_o$ (compare Figs. 2 and 6) and at θ = π/4 (same radial coordinate, r_o). The calculated values were fitted to data points accessible to gaussmeter measurements.

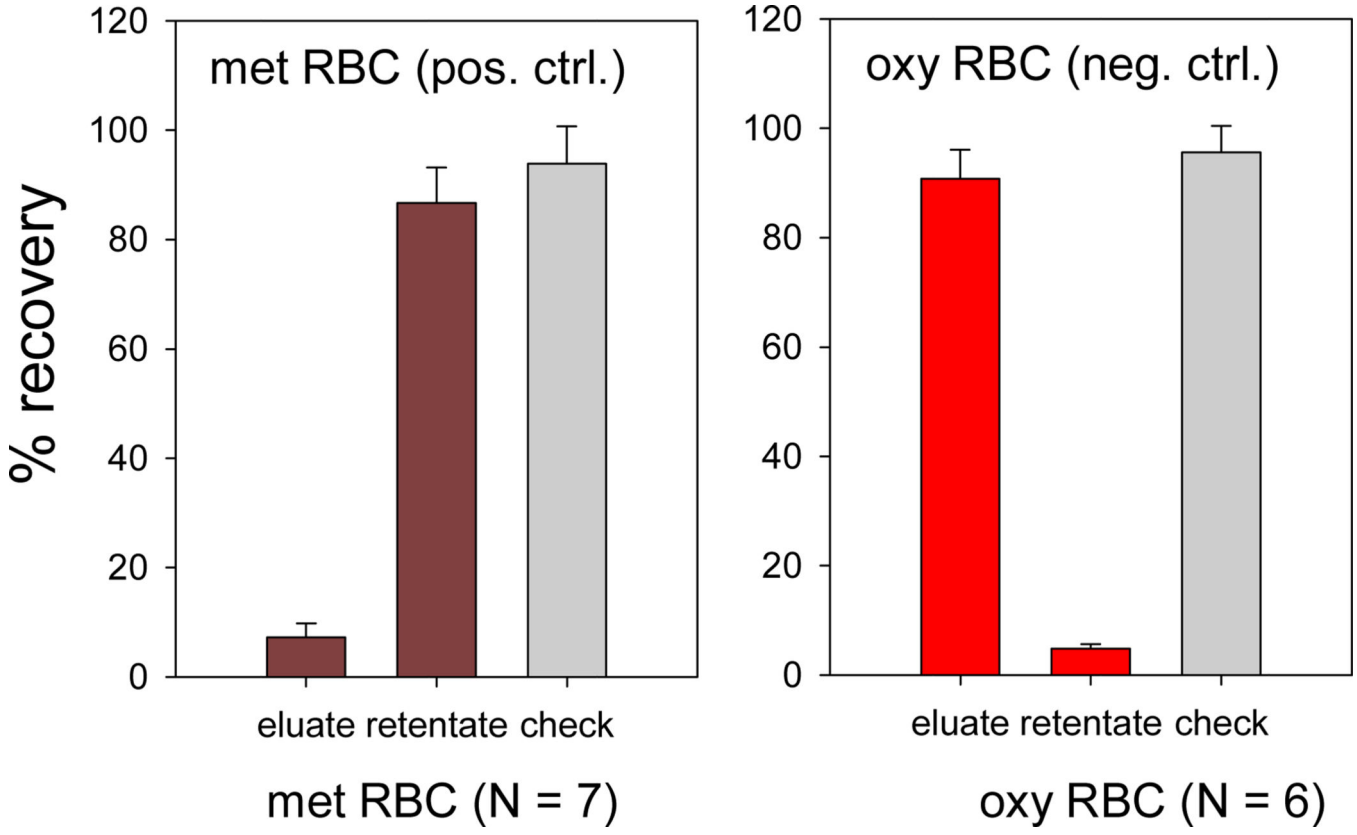

Fig. 8.

Paramagnetic methemoglobin RBC (“met RBC”, left) served as a positive control for the magnetic cell separation, and were recovered mostly in the magnetic “retentate” fraction. Oxygenated RBCs (“oxy RBC, right) served as a negative control and were separated in the nonmagnetic “eluate” fraction, as expected. The cell number balance pre- to post- separation showed nearly complete cell recovery from both fractions (“total” grey columns). The small cell losses to the other fraction were attributed to incomplete conversion of the hemoglobin to its desired form used for the experiment. The error bars indicate one standard deviation.

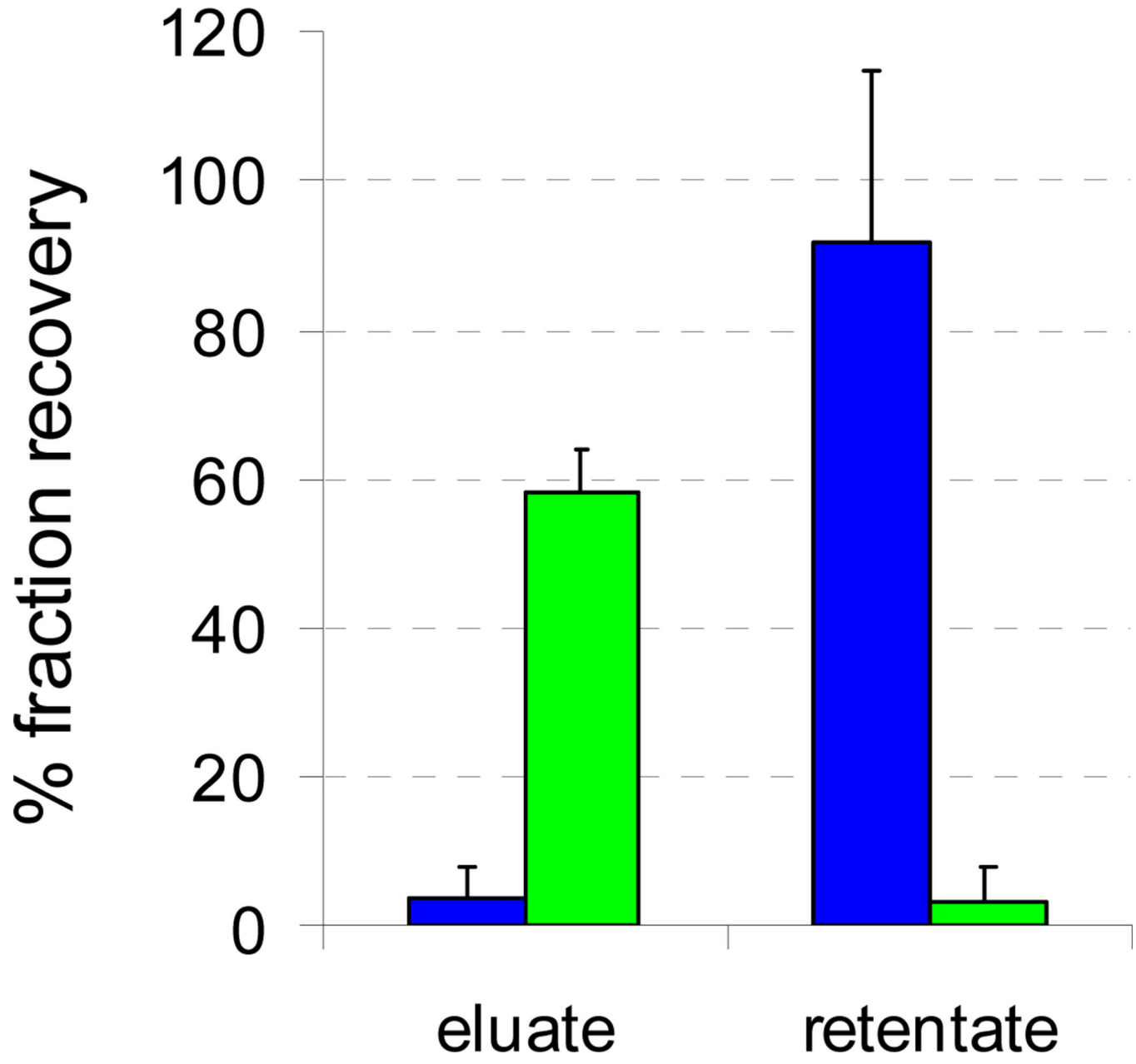

Fig. 9.

Separation of RBC (blue) from deoxygenated 50:50 mixture with Kg-1a cell line (green), by sequential elution from the magnet; recovering first, the Kg-1a cells at low flow rate (eluate) followed by the RBCs at high flow rate (retentate). The total cell number concentration was 0.5×10^{8}/mL, n = 5. The noticeable Kg-1a cell losses in the system were attributed to their sedimentation. The error bars indicate one standard deviation.

TABLE I

Magnetic RBC Sorter Design Parameters

Symbol	Quantity	Value
B	magnetic flux density	1.55 T (maximum)
dB/dr	magnetic field gradient	1,620 T/m
m	magnetophoretic mobility	4.06×10^{-6} mm^3·s/kg
u_m	field-induced RBC velocity	2.5 μm/s
χ_{RBC} (oxy)	RBC magnetic susceptibility [SI]	-9.22×10^{-6}
χ_{RBC} (deoxy)	RBC magnetic susceptibility [SI]	-5.72×10^{-6}
χ_{H2O}	water magnetic susceptibility [SI]	-9.04×10^{-6}
p_m	magnetic pressure on RBC	~ 1 Pa (maximum)
η	water viscosity	1×10^{-3} Pa·s
r_o	external cylinder radius	0.90 mm
r_i	internal cylinder radius	0.66 mm
L	magnet length	76 mm
A	annular channel cross section area	1.15 mm^2
Q	volumetric flow rate	0.05 to 2 mL/min
V_s	Sample volume	0.020mL